Design and Construction of Charged Particle Telescope Array for Study of Exotic Nuclear Clustering Structure[*]

Zheng-Li Liao,[1, 2] Xi-Guang Cao,[3, 1, 2, †] Yu-Xuan Yang,[1, 4] Chang-Bo Fu,[5] and Xian-Gai Deng[5, 6]

[1]*Shanghai Institute of Applied Physics, Chinese Academy of Sciences, Shanghai 201800, China*
[2]*University of Chinese Academy of Sciences, Beijing 100049, China*
[3]*Shanghai Advanced Research Institute, Chinese Academy of Sciences, Shanghai 201210, China*
[4]*Zhengzhou University, Zhengzhou 450001, China*
[5]*Key Laboratory of Nuclear Physics and Ion-beam Application (MOE),*
Institute of Modern Physics, Fudan University, Shanghai 200433, China
[6]*Shanghai Research Center for Theoretical Nuclear Physics NSFC and Fudan University, Shanghai 200438, China*

The exploration of exotic shapes and properties of atomic nuclei, e.g., α cluster and toroidal shape, is a fascinating field in nuclear physics. To study the decay of these nuclei, a novel detector aimed at detecting multiple alpha-particle events was designed and constructed. The detector comprises two layers of double-sided silicon strip detectors (DSSD) and a cesium iodide scintillator array coupled with silicon photomultipliers array as light sensors, which has the advantages of their small size, fast response, and large dynamic range. DSSDs couple with cesium iodide crystal arrays are used to distinguish multiple alpha hits. The detector array has a compact and integrated design that can be adapted to different experimental conditions. The detector array was simulated using Geant4, and the excitation energy spectra of some alpha-clustering nuclei were reconstructed to demonstrate the performance. The simulation results show that the detector array has excellent angular and energy resolutions, enabling effective reconstruction of the nuclear excited state by multiple alpha particle events. This detector offers a new and powerful tool for nuclear physics experiments and has the potential to discover interesting physical phenomena related to exotic nuclear structures and their decay mechanisms.

Keywords: cluster decay, toroidal structure, telescope array, SiPM, energy resolution

I. INTRODUCTION

The study of exotic shapes of nuclei is an exciting field that has opened new avenues of research in nuclear physics. Understanding the shapes of nuclei is crucial for gaining insight into the underlying physical phenomena governing the nuclear structure and behavior. When nuclei are excited to high energies or exhibit a high angular momentum, they can exhibit a variety of exotic shapes, such as linear-chain, toroid, cylinders, and bubbles, which are not emerge under normal conditions. The toroidal structure of the nucleus was first proposed by Wheeler [1]. Wong systematically studied the conditions for the existence of toroidal nuclei in medium-and heavy-mass regions [2–4] and light-mass regions [5, 6]. Recently, various sophisticated Hartree-Fock (HF) microscopic methods have addressed the issue of light toroidal nuclei [7, 8]. These theoretical studies suggest that these exotic shapes arise because of the interplay between nuclear, centrifugal, and Coulomb forces. Exotic resonance peaks at very high predicted excitation energies in the 7α disassembly of ^{28}Si were recently observed, which matched well with the excitation energy of the toroidal nuclei [9–12], indicating the successful population and detection of toroidal high-spin isomers.

The Hoyle state has important implications for the nuclear reactions and nucleosynthesis processes that occur in stellar environments. ^{8}Be and ^{12}C nuclei exhibit distinct cluster structures, such as the well-known Hoyle state of ^{12}C and the $\alpha + ^{2}n + ^{2}n$ cluster structure of ^{8}He, which closely resemble the 3α-condensate-like structure of the Hoyle state [13]. The Hoyle state is the key to understanding the nature of nuclear forces and nuclear structures. Besides, some studies have demonstrated the emergence of a π-bond linear-chain molecular rotational band in ^{14}C [14]. Recently, new evidence for a predicted Hoyle-like structure in ^{16}O was found [15]. Research on multiple clustering configurations in ^{24}Mg yielded significant results [16]. In addition, typical clustering structures in ^{12}Be and linear-chain clustering structures in neutron-rich ^{16}C have been observed [17, 18], indicating that clustering is a general phenomenon observed in light nuclei [19–22]. Therefore, it is plausible to assume that heavier conjugate nuclei have similar cluster states.

The excited states of clustering and toroidal nuclei tend to form exotic shapes that can decay into multiple alpha clusters. Experimental investigation of nuclei with alpha-cluster states requires the precise measurement of multiple alpha particles emitted during the decay process [23, 24]. To study these phenomena, advanced experimental techniques have been developed that can fit the requement of the measurement of multiple alpha-particle events with high resolution.

[†] Corresponding author, CAO xiguang, Email:caoxg@sari.ac.cn

The coincident detection of these particles reveals crucial insights into the fragmentation process of nuclei, which helps in understanding the underlying physics of the nuclear structure and decay mechanism. Several detectors have been specifically developed for measuring multiple alpha waves and have been used in various research facilities worldwide. One method of studying nuclear reactions involving multiple alpha particles is to use detectors that can measure the energy and direction of each alpha particle. The Cylindrical Array for Tracking and Spectroscopy (CATS) in the Grand Accélérateur National d'Ions Lourds (GANIL) consists of two low-pressure multiwire proportional chambers that can detect and identify alpha particles at a high counting rate [25]. A state-of-the-art 4π array of charged-particle detectors called ChAKRA works at the Variable Energy Cyclotron Center, which facilitates high-resolution charged-particle reactions and spectroscopy studies [26]. The FAZIA can detect the Fermi energy domain of charged particles based on three telescope stages [27]. CSHINE, a detector for studying the state of asymmetrical nuclear matter, can offer opportunities for experimental studies on the collision dynamics and nuclear equations of state in heavy-ion reactions at Fermi energies [28]. Peking University teams performed calibration tests on two annular detector arrays and produced outstanding results in discriminating light-charged particles [29].

The measurement of multiple α particles is a hot topic in nuclear physics because it can provide new insights into the exotic structure and dynamics of the nuclei. Multiple α particles from clustering nuclei decay are challenging to measure owing to the limitations of the solid-angle covering and low reaction cross-section. High-resolution and high-sensitivity detectors are required to reconstruct the breakup process of nuclei that emit multiple α-particles. However, these detectors are rare and expensive, and they must deal with a large amount of background information that can obscure rare events of interest. Therefore, new methods are required to reduce background interference and enhance the signal-to-noise ratio [30–32]. The development of specialized detectors and innovative data analysis techniques is essential for advancing this field of research. Recently, machine learning methods have been used to study and analyze Hoyle states [33, 34] and clustering structures [35], which can be used to classify and predict experimental data. The future of this field lies in the design of compact and dedicated detectors that can address specific experimental difficulties and challenges, particularly in sophisticated experiments used to explore interesting clustering phenomena in nuclei [36–39]. The following sections introduce the specific structure and detection performance of the detector in terms of design, construction, simulation, and measurement.

II. DESIGN AND CONSTRUCTION

The detector consists of two layers of double-sided silicon strip detectors (DSSDs) and CsI detectors with a frame arranged to maximize the sensitive area for particle collection and detection. Frame design is crucial, as shown in Fig. 1. Telescope arrays are built with aluminum frames because aluminum is low-cost, lightweight, and the reaction and activation cross sections of aluminum are low; therefore, the impact on detection is small. Therefore, the front frame of the cesium iodide is made of high-purity aluminum.

The overall detector structure can be broadly divided into four parts. As shown in Fig. 1, the gap between the two DSSDs of type BB7 is 10 mm. To prevent the DSSDs from being damaged by the tension of the Kapton cables, four aluminum pads are attached to secure the Kapton cables.

A custom-made frame fits the trapezoidal CsI tightly and protects it from damage. The frame also contains a slot for the signal wire of the DSSDs. The cesium iodide crystal is sandwiched between a reflective layer and an aluminized film on the front surface to collect light.

The optoelectronic conversion readout model consists of 25 silicon photomultipliers (SiPMs) and their power supply and control circuits. Each SiPM is attached to a CsI crystal. The frames ensure that the SiPM and CsI are well aligned so that the scintillation from the CsI can be collected and converted into a charge signal by the SiPM as much as possible. The frames also provide mechanical support and stability to the module and prevent the CsI from sliding out of position. The SiPM signal readout model incorporates a temperature feedback circuit that can correct the signal amplitude due to the temperature shift.

The signals from the four 34-channel signal cables from DSSDs and 25-channel signal lines from SiPMs are collected using a circuit board connected to the electronics analysis module. The 25-channel signal lines are split into common 16-channel signal cables that can match various data acquisition modules.

A. Detectors

In particular, a Si-CsI combination detector for multiple α particle coincidence measurements can detect the energy and position of multiple α particles with high precision [40–42]. This can help to explore the fundamental laws of nature governing the interactions of these particles. This design utilizes 25 CsI crystals, each of which is a sloping ridge with a hypotenuse pointing towards the collision center, causing the α particles to deposit energy in only one crystal. The front and rear sides of each crystal measured 12.96×12.96 mm^2 and 15.16×15.16 mm^2, respectively, at a height of 50 mm. The 5×5 CsI crystals were sandwiched between TeO$_2$ for good reflection and combined into the frustum of a square pyramid with dimensions of 66×66 mm^2 on the front side and 77×77 mm^2 on the rear side. An array of 25 CsI crystals was machined from a large
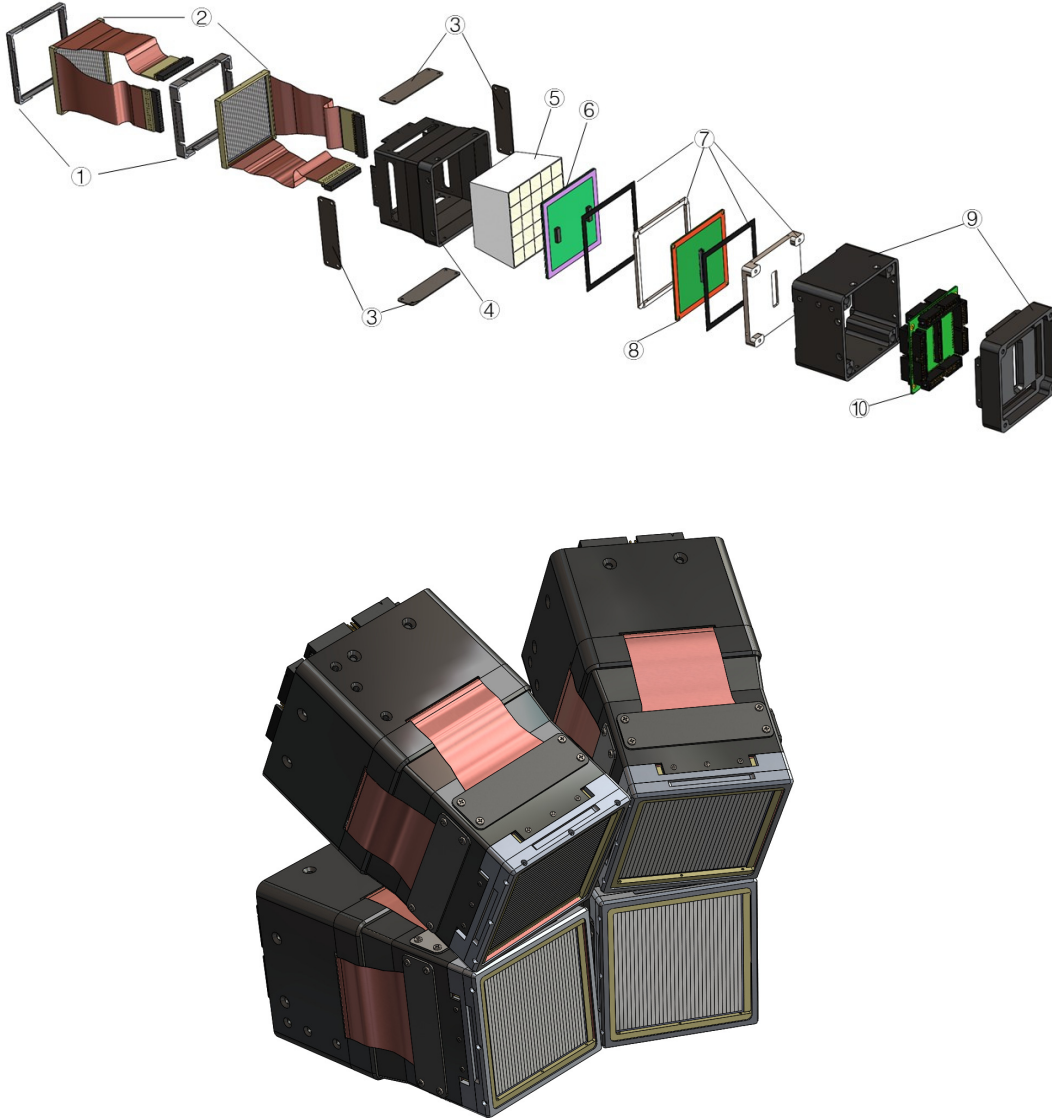
Fig. 1. Exploded view of the charged particle detector and the view of the telescope array

piece of crystal to ensure that their physical properties were similar, and TiO_2 was sandwiched between the crystals to act as a reflection layer and glue them together. This design renders the telescope array robust and compact.

The detector consists of three layers: two DSSDs and a CsI scintillator. The BB7-type DSSD from Micron Semiconductor Ltd was used to measure the position and energy loss of the incident particles. BB7 type DSSD, which has a larger sensitive area and narrower strips than the W1 type, has an active area of 63.96×63.96 mm, which consists of 32 strips, approximately 2 mm wide, on each side. DSSDs with thicknesses of 300 mm, 500 mm, and 1000 mm were purchased depending on the experimental requirements. This type of detector is suitable for high-resolution measurement of charged particles. Heavy ions deposit full energy in the DSSDs, whereas lighter particles such as alpha punch through the DSSDs and hit the CsI, where the residual energy is deposited. This configuration allows the detector to identify and locate multiple alpha particles simultaneously, which is suitable for various applications that require a high angular resolution for charge particle detection.

The semiconductor material of the Si detector forms a p-n junction, which makes it highly sensitive to charged particles. The detector can also locate the position of the particle interaction within the detector with a high spatial resolution, which is essential for accurately distinguishing multiple hit events. Moreover, the detector has a low threshold level that allows the detection of very low-energy particles.

By combining the signals from both layers of DSSD and applying kinematic judgments, the particle momentum can be

accurately determined. The hit position can also be used in conjunction with the final CsI scintillator array to reduce uncertainty in the direction of the particle momentum. This can significantly improve the accuracy of particle momentum determination by reducing the effects of multiple hits and detector resolution.

A DSSD with two layers allowed us to obtain multiple values of energy or energy loss for each particle combined with the CsI array. This enables us to identify the type of particle using the $\Delta E - E$ method.

The Si-CsI detector is a versatile device that can be used for multi-alpha-particle detection. It combines the advantages of a Si detector, which can determine the position and energy of the particles with high precision, and a CsI scintillator. The SiPM is a key component of the detector, as it has high sensitivity and a fast response time, allowing for accurate detection and measurement of low-energy particles [43–45]. SiPMs coupled with scintillator crystals such as lutetium–yttrium oxyorthosilicate and LaBr3(Ce) crystals have been highly sought after in various fields [46, 47]. The combination of SiPMs and CsI exhibits favorable characteristics in terms of detection performance. The high sensitivity and small size of SiPMs enable detectors to achieve high spatial resolution and precise energy measurements. In addition, SiPMs have good single-photon resolution, providing high-precision photon counting and particle identification capabilities.

One challenge in using DSSD is the possibility of multiple alpha particles simultaneously hitting the DSSD. The combination of the X position from the front side and Y position from the back side will lead to a multi-value for position measurement if more than one particle hits the DSSD, which makes it difficult to accurately calculate the momentum of the particle. To overcome this issue, an additional layer of DSSD can be used to obtain multi-channel signals and striking positions. Using a two-layer DSSD provides an additional set of positional information (other X and Y positions). The real hit position should be on the same line as the reaction center, which is the target. Based on this, we can determine the real positions of double-hit events.

SiPMs are ideal for compact detectors owing to their high integration and small size. Previous studies have indicated that the spectral response of SiPMs is compatible with their CsI emission spectra. Because the SiPM+CsI can detect γ, it can be used as a portable dosimeter for environmental dose equivalent and environmental dose rate equivalent measurements [45]. The combination used for proton detection consists of well-separated protons and deuterons at energies below 12 MeV. [48]. Using the Pulse Shape Discrimination (PSD) method, α particles can be easily separated from β-γ [51, 52]. In addition, the CsI crystal coupled to the SiPM was used to detect α particles and low-energy protons and was tested using the Tandem Van-der-Graff of the INFN-Laboratori Nazionali del Sud (LNS) [49]. Thus, it can be inferred that the CsI-SiPM combination can also be applied in heavy-ion collision experiments. SiPMs are high-performance detectors that detect and amplify single-photon signals. The advantages of SiPMs over conventional photomultiplier tubes (PMTs) are manifold, such as high photon detection efficiency, single photon sensitivity, fast response time, low operating voltage, low power consumption, and small size. They also have good radiation and magnetic resistance, which make them adaptable to various environments and conditions. Therefore, using SiPMs as back-end photoelectric signal conversion devices for CsI can enhance detection capabilities by enabling efficient light signal readout and processing.

III. SIMULATION

Geant4 provides a toolkit to simulate the detection process, which offers various models for physical processes such as elastic scattering, inelastic scattering, ionization, and trajectory refinement. These models are essential for studying the interactions between particles and different materials in a detection design. Geant4 also allowed us to define the complex detector geometries in detail. This enabled us to accurately model the detector and evaluate its performance.

The experimental results showed that the kinetic energy of α from the ^{28}Si breakup was lower than 300 MeV [10]. Alpha particles with energies below 520 MeV can be fully stopped in a 50 mm CsI crystal. Therefore, the energy of α particles can be measured using a CsI crystal. Furthermore, alpha-conjugate nuclei with higher masses, such as ^{12}C, ^{16}O, ^{20}Ne, and ^{24}Mg, are mostly stopped in DSSDs. Therefore, the experiment can detect the light and heavy particles of interest simultaneously.

A. Angular Resolution

The DSSDs can provide the position information of the particle hitting the detector, and the θ and ϕ values of the particle emissions can be calculated using this position information. Assuming that the Z-axis is the direction of the incident particle beam, θ and ϕ can be obtained as follows:

$$\theta = arctan(\frac{\sqrt{x^2 + y^2}}{z}) \tag{1}$$

$$\phi = arctan(\frac{y}{x}) \tag{2}$$

where x, y, z are the position information obtained from the DSSDs.

Angle resolution is crucial for the performance of the system. To evaluate the desired angular resolution, we select several discrete values of θ and ϕ. The distance between the target and the detectors, which was 150 mm, was chosen to cover a forward angle of up to $\pm 25°$. The distribution of θ without ϕ restriction is shown in Fig. 2(a). The detectors can cover a ϕ angle from $0°$ to $360°$, except for the gaps between the telescope arrays. The ϕ-distribution is shown in Fig. 2(b).
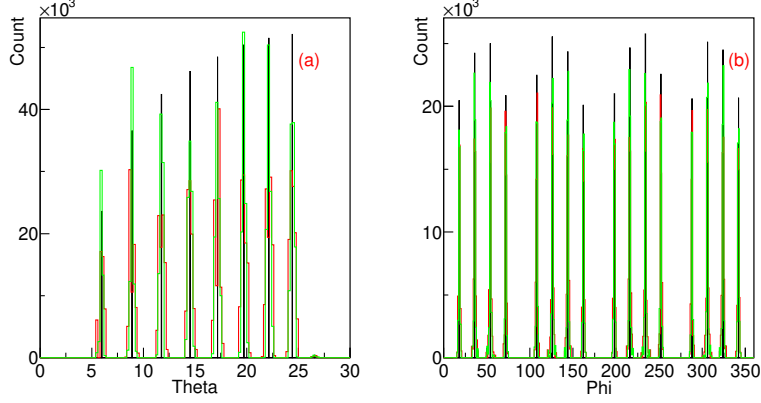

Fig. 2. Distribution of α particles. Panels (a) and (b) show the θ and ϕ resolutions of the telescope array, which is placed 15 cm away from the target. Black curve represents the input value of the simulation, and the red and green curves represent the angular distribution calculated with single DSSD and double layer DSSDs, respectively.

As Fig. 2 shows, the FHWM of angular resolution for θ ranges from $0.2°$ to $0.4°$, whereas the FHWM of angular resolution for ϕ is approximately $2.2°$. The measurements of θ and ϕ show a noticeable difference in the angular resolution capability between the single DSSD and double-layer DSSD. The double-layer DSSD performs better in terms of angular resolution capability. These angular-resolution capabilities affect the reconstruction of fragmented nuclei during multiple alpha events. Hence, the use of two layers of DSSD enables more precise event reconstruction. The next section illustrates the differences in the reconstruction of the particle excited states between single- and double-layer DSSDs.

B. Event Reconstruction

By collecting and analyzing the data of the particles emitted from the nuclear collision process, we can infer the dynamics and nuclear state of the collision event. Event reconstruction is a crucial technique that allows physical information to be drawn from data. The performance and accuracy of event reconstruction are essential parameters affecting the performance of charged-particle telescope arrays.

The outcome of low-energy particle collisions can be characterized by several parameters, such as the excitation energy of the fragment before it decays and the angular distribution of the fragment. These parameters provide valuable information on the dynamics and mechanisms of the collision process, as well as the properties and structures of the particles and fragments involved. Therefore, it is essential to measure and analyze the experimental parameters of low-energy particle collisions. Important and interesting physical parameters, such as E_x denote the excitation energy of the projectile nuclei, and E_{tot} denotes the total kinetic energy of all fragments in the laboratory frame.

$$E_x = \sum K_{c.m.} - Q \tag{3}$$

and

$$E_{tot} = \sum K_{lab} + K_{recoil} \tag{4}$$

where $K_{c.m.}$ denotes the kinetic energy in the center-of-mass frame of the summed particles. Q is the Q-value of a nuclear reaction, which represents the difference between the masses of the initial reactants and final products. K_{lab} denotes the kinetic energy in the laboratory frame, and K_{recoil} represents the kinetics of the recoil nuclear energy calculated by the conservation of energy and momentum.

This information is crucial for gaining a more comprehensive understanding of the physical processes underlying an experiment. By combining the cascade decay process, we can gain insights into the fundamental properties of the particles involved

as well as the energy distribution and dynamics of the system as a whole. In addition, according to the charge multiplicity distribution, the temperature of the heavy-ion collisions can be determined, which can be applied to analyze the reaction dynamics [50].

This spectrum from ^{28}Si fragmented into 7 α particles [10] was used as an input for Geant4 simulation to model the detection process, and the alpha particles hit the detectors event-by-event. Such simulations are more realistic and allow for better evaluation and analysis of the performance of the detector under experimental conditions. However, based on these data, it is estimated that approximately 20% of the 7 alpha events may be lost because of the detection geometry efficiency.
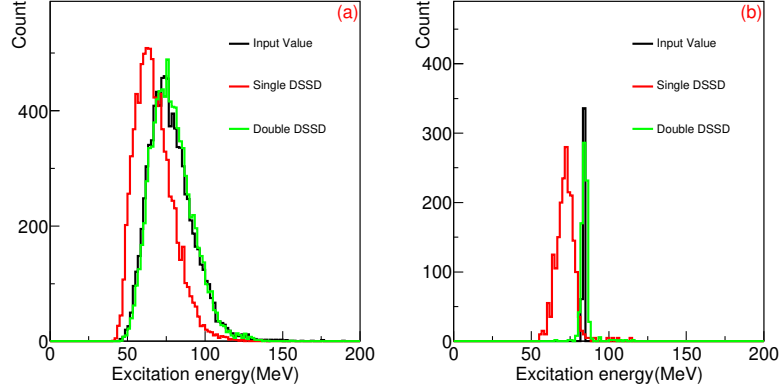

Fig. 3. Panel (a) shows the excitation energy distribution of ^{28}Si reconstructed by 7 α particles. The panel (b) shows the distribution with a restriction on the input value between 83 MeV and 85 MeV.

Fig. 3 shows the excitation energy distribution of ^{28}Si reconstruction from 7 α. It is evident that the calculated result with double DSSDs matches the simulated input. A single DSSD shows poor performance for the 7 α events. Because some events respond simultaneously on multiple silicon strips, this can interfere with the position resolution of a single DSSD, whereas double DSSDs can eliminate such effects through momentum analysis.

This array of charged-particle detectors was specially designed and optimized for alpha particle detection. It can detect the 7 α particle events that occurred in the experiment, as well as the fragmentation of alpha-conjugated nuclei into N alpha events. By analyzing the data from these events, we can reconstruct the excitation energies of the nuclei.

One possible explanation for the occurrence of 7 α particles might be the cascade decay of ^{28}Si, which means that the decay product may contain other alpha-conjugated nuclei, such as ^{8}Be and ^{12}C. To investigate this hypothesis, the data from the alpha-conjugated nuclei should be analyzed. Reconstructing the cascade decay process of ^{28}Si to understand how it produces 7 α particles is a novel approach for studying the nuclear structure and dynamics of ^{28}Si and its decay products.

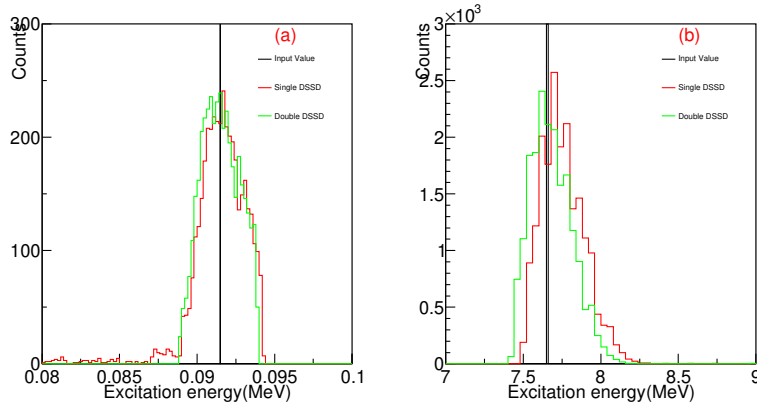Fig. 4. Excitation energy distribution of ^{8}Be breaks up to 2 α particles and ^{12}C breaks up to 3 α particles.

The excitation energy of ^{8}Be is low, and the 2 α particles from the decay have a very small emission angle in collisions, which requires a high angular resolution to detect the 2 α event. ^{8}Be nuclei will be produced in large numbers in the reaction, indicating that there is a high rate of double-alpha hit events in the experiment. Therefore, it is important to simulate how the

detector responds to the fragmentation events of ^{8}Be. Fig. 4.(a) depicts the excitation energy spectra of ^{8} reconstructed using 2 α-particles. When 2 α hit the detector simultaneously, two sets of X-Y values are obtained, corresponding to two sets of spatial positions. The single-layer DSSD cannot distinguish the real position of α hit, which causes the result to deviate from the input value. Double-layer DSSDs provide another set of spatial positions from which the hit position can be determined through momentum analysis. In addition to ^{8}Be, ^{12}C can also be produced during the reaction. The production of ^{12}C in stars via the triple-alpha process depends on a specific resonance of ^{12}C, called the Hoyle state. This resonance has important implications for nuclear structure theory and nuclear astrophysics applications. It is essential to evaluate the ability of the detectors to reconstruct the ^{12}C fragmentation events that occur in the Hoyle state. The simulation results are presented in Fig. 4(b). In the simulation for reconstructing ^{12}C, the double-layer DSSDs outperformed the single-layer DSSD. As shown in Fig. 4, the charged-particle telescope array reconstructs the excitation energies of ^{8}Be and ^{12}C with reasonable accuracy. The alpha particles derived from the double-layer DSSD provided more accurate excitation energies than those derived from the single-layer DSSD. Therefore, a double-layer DSSD design is required for this purpose.

Moreover, the results demonstrate that the telescope array is versatile and suitable for various experiments, in addition to those involving the disintegration of ^{28}Si into 7 α particles. It can also achieve good performance in experiments that generate multiple alpha particles or multiple fragments of different masses, owing to its high-angle resolution.

The telescope array exhibited remarkable performance and accuracy in the excitation energy spectra of the reconstructed nuclei. Thus, it is a vital tool for studies involving these processes.

IV. MEASUREMENT

The simulation results indicate that the detector meets the performance requirements of the experiment; however, further validation is necessary to assess its actual performance. At present, the evaluation of the capability of the detector to detect charged particles is limited to the use of an ^{241}Am source. The decay of ^{241}Am primarily produces alpha particles with an energy of 5.486 MeV. These particles have a low penetration depth and can be blocked using a single-layer DSSD. Therefore, the energy resolution can be determined separately for the DSSD and CsI components. The energy resolution of the cesium-iodide scintillation detector was measured.
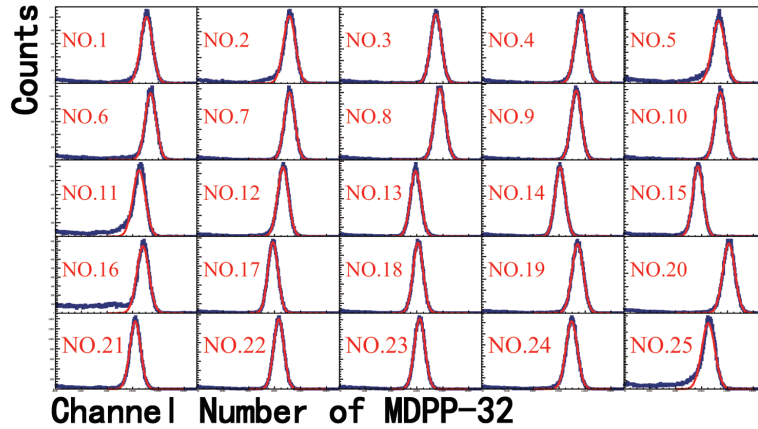

Fig. 5. Test results of 25 CsI+SiPM detectors with the ^{241}Am α source. The data points are fitted with a Gaussian function.

The energy spectrum of the telescope array consists of 25 CsI crystals coupled to 25 SiPMs with a 30 V voltage and gain of 20 on the operation amplifier circuit, as shown in Fig. 5. It can be seen that there are small differences in performance for CsI crystals. This may be due to the variation in the alpha spectra because of the heterogeneity of the CsI crystals, although they are from one large block of CsI. In addition, the position of the radioactive source during the measurement may influence the results.

Fig. 6 shows that the energy resolution is approximately 9%. Compared with the traditional design, sandwiched TiO$_2$ can achieve comparable energy resolution [51, 52].

According to Fig. 7, the energy resolution of the CsI+SiPM composite detector depends on the voltage applied to SiPM. A higher voltage results in a higher gain, a smaller dynamic range, and better energy resolution. However, when detecting a particle with high energy, the increased noise and saturation effects caused by high voltage can affect the detector resolution. To detect high-energy, even up to 300 MeV alpha particles, the voltage applied to SiPM should be set as low as possible. However, the overall performance of the telescope array for high-energy particles, including the energy resolution, crosstalk, and charged-particle identification capability, must be assessed by performing online beam tests.
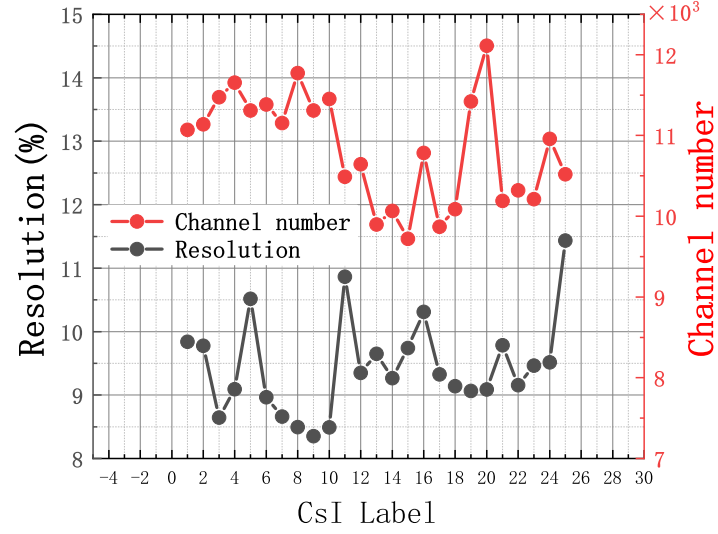
Fig. 6. Test results of 25 CsI+SiPM detectors. Channel number is the readout.
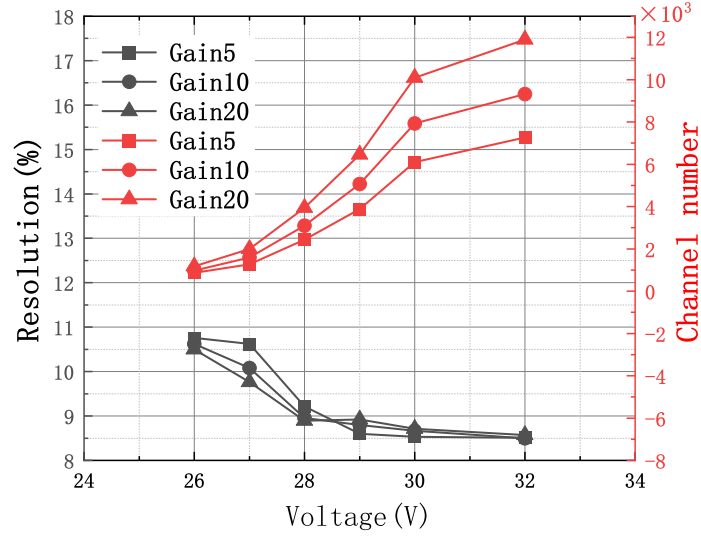

Fig. 7. Performance of the CsI+SiPM detector under different operating conditions. Channel numbers (red line) and energy resolution (black line) depend on the voltage applied to the SiPM. Channel number is the readout from MDPP-32.

V. SUMMARY

A novel detector array consisting of two DSSDs and a 5×5 cesium iodide scintillator array coupled with a SiPM array for particle identification and tracking of particle trajectories was designed and tested aiming at the detection of multiple α particle events with high position resolution. The high sensitivity and excellent timing performance of SiPM make it a good light signal readout module. CsI+SiPM detectors can be used in experiments to detect protons or deuterons with low energy. However, this is the first attempt to use the CsI+SiPM array to detect high-energy particles in heavy-ion collisions. The compact and robust telescope array is suitable for various experimental scenarios owing to the small size of SiPM and the sandwiching technology applied for CsI array.

Using the Geant4 tookit, the detector responses to α particles with different energies and angles have been simulated. The simulation results indicate that the detector array has high angular and energy resolutions, enabling accurate distinguishing of multiple α particle events. Additionally, the reconstruction result of ^{28}Si excitation energy using 7 α is satisfactory. This telescope array coupled with SiPM is a novel design for nuclear physics experiments, which can be used not only in experiments investigating exotic toroidal structures but also in future experiments to study the excitation states involving nuclear clusters, contributing to the exploration of the decay and dynamics of exotic nuclear shapes.

[1] J. A. Wheeler, Nucleonics Notebook, 1950 (unpublished), see also p. 297 in G. Gamow, Biography of Physics, Harper & Brothers Publishers, N. Y. 1961; Princeton University Graduate Course Physics 576 Take-Home Examination Problem 2, May 22, 1963 (unpublished).

[2] A.Kosior, A.Staszczak, CY Wong C.Y. Wong, Toroidal Nuclear Matter Distributions of Superheavy Nuclei from Constrained Skyrme-HFB Calculations. Oak Ridge National Lab.(ORNL), Oak Ridge, TN (United States), 2017. https://doi.org/10.5506/APhysPolBSupp.10.249

[3] C.Y. Wong, Toroidal nuclei. Phys. Lett. B **41**, 446-450 (1972). https://doi.org/10.1016/0370-2693(72)90671-5.

[4] C.Y. Wong, Toroidal and spherical bubble nuclei. Ann. Phys. **77**, 279-353 (1973). https://doi.org/10.1016/0003-4916(73)90420-X

[5] C.Y. Wong, Rotating toroidal nuclei. Phys. Rev. C **17**, 331 (1978). 10.1103/PhysRevC.17.331

[6] C.Y. Wong, Hot toroidal and bubble nuclei. Phys. Rev. Lett **55**, 1973 (1985). https://doi.org/10.1103/PhysRevLett.55.1973

[7] Staszczak. A, C.Y. Wong, A region of high-spin toroidal isomers. Phys. Lett. B **738**, 401-404 (2014).https://doi.org/10.1016/j.physletb.2014.10.013.

[8] T. Ichikawa, J.A. Maruhn, N. Itagaki, et al, Existence of an Exotic Torus Configuration in High-Spin Excited States of Ca 40. Phys. Rev. Lett. **109**, 232503 (2012). DOI:https://doi.org/10.1103/PhysRevLett.109.232503

[9] X.G. Cao, E.J. Kim, K. Schmidt, et al., Examination of evidence for resonances at high excitation energy in the 7 α disassembly of ^{28}Si. Phys. Rev. C **99**, 014606 (2019). DOI:https://doi.org/10.1103/PhysRevC.99.014606

[10] X.G. Cao, E.J. Kim, K. Schmidt, et al., α and α Conjugate Fragment Decay from the Disassembly of ^{28}Si at Very High Excitation Energy. JPS. Conf. Proc. **32**, 010038 (2020). DOI:https://doi.org/10.7566/JPSCP.32.010038

[11] X.G. Cao, E.J. Kim, K. Schmidt, et al., Evidence for resonances in the 7 α disassembly of ^{28}Si. AIP. Conf. Proc. **2038**, 020021 (2018). DOI:https://doi.org/10.1063/1.5078840

[12] Z.X. Ren a, P.W. Zhao a, S.Q. Zhang, et al., Toroidal states in 28Si with covariant density functional theory in 3D lattice space. Nucl. Phys. A **996**, 121696 (2020). DOI:https://doi.org/10.1016/j.nuclphysa.2020.121696

[13] Z.H. Yang, Y.L. Ye, B. Zhou, et al., Observation of the Exotic 0^{2+} Cluster State in ^{8}He. Phys. Rev. Lett. **131**, 242501 (2023).DOI:https://doi.org/10.1103/PhysRevLett.131.242501

[14] J.Han, Y. Ye,J. Lou, et al., Nuclear linear-chain structure arises in carbon-14. Commun. Phys. **6**, 220 (2023).DOI:https://doi.org/10.1038/s42005-023-01342-6

[15] J.H. Chen, Y.L. Ye, K. Ma, et al., New evidence of the Hoyle-like structure in ^{16}O. Sci. Bull. **68**, 1119-1126 (2023). https://doi.org/10.1016/j.scib.2023.04.031

[16] D.X. Wang, Y.L. Ye, C.J. Lin, et al., α-cluster decay from 24Mg resonances produced in the ^{12}C (^{16}O, ^{24}Mg) α reaction. Chin. Phys. C **47**, 014001 (2023). DOI 10.1088/1674-1137/ac9e9a

[17] Z.H. Yang, Y.L. Ye, Z.H. Li, et al., Observation of Enhanced Monopole Strength and Clustering in ^{12}Be. Phys. Rev. lett. **112**, 162501 (2014). https://doi.org/10.1103/PhysRevLett.112.162501

[18] Y. Liu, Y.L. Ye, J.L. Lou, et al., Positive-Parity Linear-Chain Molecular Band in ^{16}C. Phys. Rev. Lett. **124**, 192501 (2020). https://doi.org/10.1103/PhysRevLett.124.192501

[19] Y. Liu, Y.L. Ye, Nuclear clustering in light neutron-rich nuclei. Nucl. Sci. Tech. **29**, 184 (2018). DOI: 10.1007/s41365-018-0522-x

[20] R. Bijker, F. Iachello, Cluster structure of light nuclei. Prog. Part. Nucl. Phys. **110**, 103735 (2020). DOI: 10.1016/j.ppnp.2019.103735

[21] M. Freer, H. Horiuchi, Y. Kanada-En'yo, et al. Microscopic clustering in light nuclei. Rev. Mod. Phys. **90**, 035004 (2018). DOI: 10.1103/RevModPhys.90.035004

[22] T. Ichikawa, JA. Maruhn, N. Itagaki et al., Linear Chain Structure of Four-α Clusters in ^{16}O. Phys. Rev. Lett. **107**, 112501 (2011). https://doi.org/10.1103/PhysRevLett.107.112501

[23] M. Barbui, K. Hagel, VZ. Goldberg, et al., Exploring the alpha cluster structure of nuclei using the thick target inverse kinematics technique for multiple alpha decays. EPJ. Web. Conf. **66**, 03005 (2014). DOI:https://doi.org/10.1051/epjconf/20146603005

[24] J. Bishop, T. Kokalova, M. Freer, et al., Experimental investigation of α condensation in light nuclei. Phys. Rev. C **100**, 034320 (2019). DOI:https://doi.org/10.1103/PhysRevC.100.034320

[25] D. Ferenc, Imaging hybrid photon detectors with minimized dead area and protection against positive ion feedback. Nucl. Instrum. Methods. Phys. Res. A **431**, 460-475 (1999). https://doi.org/10.1016/S0168-9002(99)00209-0

[26] S. Kundu, TK. Rana, C. Bhattacharya, et al., ChAKRA: The high resolution charged particle detector array at VECC. Nucl. Instrum. Methods. Phys. Res. A **943** 162411 (2019). https://doi.org/10.1016/j.nima.2019.162411

[27] G. Poggi, FAZIA: Prototyping a next-generation 4π array for nuclear reaction-dynamics studies. Eur. Phys. J. Spec. Top. **150**, 369-372 (2007). https://doi.org/10.1140/epjst/e2007-00350-1

[28] J. Wang, F.H. Guan, X.Y. Diao, et al., CSHINE for studies of HBT correlation in heavy ion reactions. Nucl. Sci. Tech. **32**, 4 (2021). https://doi.org/10.1007/s41365-020-00842-2

[29] H.Y. Zhu, J.L. Lou, Y.L. Ye, et al., Two annular CsI (Tl) detector arrays for the charged particle telescopes. Nucl. Sci. Tech. **34**, 159

(2023). DOI: https://doi.org/10.1007/s41365-023-01319-8

[30] H.K. Wu, C. Li. A ROOT-based detector test system. Nucl. Sci. Tech. **32**, 115 (2021). https://doi.org/10.1007/s41365-021-00952-5

[31] K.X. Huang, Z.J. Li, Z. Qian, et al., Method for detector description transformation to Unity and application in BESIII. Nucl. Sci. Tech. **33**, 142 (2022). https://doi.org/10.1007/s41365-022-01133-8

[32] D. Guo, Y.H. Qin, S. Xiao, et al., An FPGA-based trigger system for CSHINE. Nucl. Sci. Tech. **33**, 162 (2022). https://doi.org/10.1007/s41365-022-01149-0

[33] W.B. He, Y.G. Ma,L.G. Pang, et al., High-energy nuclear physics meets machine learning. Nucl. Sci. Tech. **34**, 88 (2023). https://doi.org/10.1007/s41365-023-01233-z

[34] H. Wu, Y. Wang, Y. Wang, et al., Machine learning method for ^{12}C event classification and reconstruction in the active target time-projection chamber. ArXiv. **2304**, 13233 (2023). https://doi.org/10.1016/j.nima.2023.168528

[35] J. He, W.B. He, Y.G. Ma, S. Zhang et al., Machine-learning-based identification for initial clustering structure in relativistic heavy-ion collisions. Phys. Rev. C **104**, 044902 (2021). https://doi.org/10.1103/PhysRevC.104.044902

[36] W.B.He, Y.G. Ma, X.G. Cao, et al., Dipole oscillation modes in light α-clustering nuclei. Phys. Rev. C **94**, 014301 (2016). https://doi.org/10.1103/PhysRevC.94.014301

[37] X.G. Cao, Y.G. Ma, Progress of theoretical and experimental studies on α cluster structures in light nuclei. Chin. Sci. Bull. **60**, 1557-1564 (2015). https://doi.org/10.1360/N972014-01335

[38] W.B.He,X.G. Cao, Y.G. Ma, Application of EQMD model to researches of nuclear exotic structures. Nucl. Tech. **37**, 100511 (2014). 10.11889/j.0253-3219.2014.hjs.37.100511

[39] W.B.He, Y.G. Ma, X.G. Cao, et al., Giant Dipole Resonance as a Fingerprint of α Clustering Configurations in ^{12}C and ^{16}O. Phys. Rev. Lett. **113**, 032506 (2014). https://doi.org/10.1103/PhysRevLett.113.032506

[40] F. Guan, Y. Wang, X. Diao, et al., Track recognition for the ΔE-E telescopes with silicon strip detectors. Nucl. Instrum. Methods. Phys. Res. A **1029**, 166461 (2022). https://doi.org/10.1016/j.nima.2022.166461

[41] W. Khan, C.H. He, Q.M. Zhang, et al., Design of CsI(Tl) detector system to search for lost radioactive source. Nucl. Sci. Tech. **30**, 132 (2019). https://doi.org/10.1007/s41365-019-0658-3

[42] Y.B. Xu, X.Q. Li, X.L. Sun, et al., The design and performance of charged particle detector onboard the GECAM mission. Radiat. Detect. Technol. Methods. **6**, 53–62 (2022). https://doi.org/10.1007/s41605-021-00298-x

[43] D. Yan, Z.Y. Sun, K. Yue, et al., Design and construction of a multi-layer CsI (Tl) telescope for high-energy reaction studies. Nucl. Instrum. Methods. Phys. Res. **843**, 5-10 (2017). https://doi.org/10.1016/j.nima.2016.10.053

[44] W. Lu, L. Wang, Y. Yuan, et al., Monte Carlo simulation for performance evaluation of detector model with a monolithic LaBr3 (Ce) crystal and SiPM array for γ radiation imaging. Nucl. Sci. Tech. **33**, 107 (2022). https://doi.org/10.1007/s41365-022-01081-3

[45] T. Teranishi, Y. Ueno, M. Osada, et al., Pulse shape analysis of signals from SiPM-based CsI (Tl) detectors for low-energy protons: Saturation correction and particle identification. Nucl. Instrum. Methods. Phys. Res. A **989**, 164967 (2021). https://doi.org/10.1016/j.nima.2020.164967

[46] Y.Y. Li, C.Y. Li, K. Hu, Design and development of multi-channel front end electronics based on dual-polarity charge-to-digital converter for SiPM detector applications. Nucl. Scie. Tech. **34**, 18 (2023). https://doi.org/10.1007/s41365-023-01168-5

[47] W .Lu, L. Wang, Y. Yuan, et al., Monte Carlo simulation for performance evaluation of detector model with a monolithic LaBr3 (Ce) crystal and SiPM array for γ radiation imaging. Nucl. Sci. Tech. **33**, 107 (2022). https://doi.org/10.1007/s41365-022-01081-3

[48] P. Buzhan, A. Karakash, Y. Teverovskiy Silicon Photomultiplier and CsI (Tl) scintillator in application to portable H*(10) dosimeter. Nucl. Instrum. Methods. Phys. Res. A **912**, 245-247 (2018). https://doi.org/10.1016/j.nima.2017.11.067

[49] M. Bondí, M. Battaglieri, M. Carpinelli, et al., Large-size CsI (Tl) crystal read-out by SiPM for low-energy charged-particles detection. Nucl. Instrum. Methods. Phys. Res. A **867**, 148-153 (2017). https://doi.org/10.1016/j.nima.2017.06.024

[50] Y.D. Song,R. Wang,Y.G. Ma, et al., Determining the temperature in heavy-ion collisions with multiplicity distribution. Phys. Lett. B **814**, 136084 (2021). https://doi.org/10.1016/j.physletb.2021.136084

[51] NVH. Viet, K. Takahisa, M. Nomachi, et al., Pulse Shape Discrimination of CsI (Tl) with Photomultiplier Tube and MPPCs. 2019 IEEE Nuclear Science Symposium and Medical Imaging Conference (NSS/MIC). 1-3 (2019). 10.1109/NSS/MIC42101.2019.9059996

[52] Viet N V H, Nomachi M, Takahisa K, et al. Pulse shape discrimination of CsI (Tl) with a photomultiplier tube and multipixel photon counters. IEEE. Trans. Nucl. Sci. **68**, 203-210 (2020). 10.1109/TNS.2020.3047615

[53] G. Stellin, S. Elhatisari, UG. Meißner, Breaking and restoration of rotational symmetry in the low energy spectrum of light α-conjugate nuclei on the lattice I: 8Be and 12C. Eur. Phys. J. A **54**, 232 (2018). https://doi.org/10.1140/epja/i2018-12671-6

[54] Zoghi-Foumani N, Shojaei M R, Rajabi A A. A new non-microscopic study of cluster structures in light alpha-conjugate nuclei. Chin.Phys. C **41**, 014104 (2017). https://doi.org/10.1088/1674-1137/41/1/014104